



# Non-Newtonian Polymer–Nanoparticle Hydrogels Enhance Cell Viability during Injection

Hector Lopez Hernandez, Abigail K. Grosskopf, Lyndsay M. Stapleton, Gillie Agmon, and Eric A. Appel\*

Drug delivery and cell transplantation require minimally invasive deployment strategies such as injection through clinically relevant high-gauge needles. Supramolecular hydrogels comprising dodecyl-modified hydroxypropyl-methylcellulose and poly(ethylene glycol)-*block*-poly(lactic acid) have been previously demonstrated for the delivery of drugs and proteins. Here, it is demonstrated that the rheological properties of these hydrogels allow for facile injectability, an increase of cell viability after injection when compared to cell viabilities of cells injected in phosphate-buffered saline, and homogeneous cell suspensions that do not settle. These hydrogels are injected at 1 mL min<sup>-1</sup> with pressures less than 400 kPa, despite the solid-like properties of the gel when at rest. The cell viabilities immediately after injection are greater than 86% for adult human dermal fibroblasts, human umbilical vein cells, smooth muscle cells, and human mesenchymal stem cells. Cells are shown to remain suspended and proliferate in the hydrogel at the same rate as observed in cell media. The work expands on the versatility of these hydrogels and lays a foundation for the codelivery of drugs, proteins, and cells.

Hydrogels' use has increased over the past 30 years in biomedical applications such as drug delivery,<sup>[1,2]</sup> bioprinting for 3D printing,<sup>[3]</sup> and cell therapies.<sup>[4,5]</sup> Hydrogels are readily suited for biological applications because of their tissue-like mechanical properties, high water content, biocompatibility,

and stimuli-responsiveness. In the field of drug delivery, hydrogels provide sustained and temporally controlled delivery of drugs in localized regions, reducing off-target toxicity and increasing clinical efficacy.<sup>[4,6–9]</sup>

Administering cells through high-gauge needles is becoming more common due to the development of cell therapies<sup>[10]</sup> and 3D bioprinting technologies<sup>[3]</sup>; however, previous studies have shown that injecting cells through clinically relevant needles often results in cell death and poor cell viability.<sup>[11]</sup> Targeted cell delivery is often desired for medical application, but the therapeutic effect of the treatment is decreased because many of the cells injected in saline solutions (i.e., phosphate-buffered saline [PBS]) are regurgitated due to the pressure in the tissue and fluid flow away from the injection site.<sup>[10]</sup>

Technology development is needed to enhance the delivery, protection, and encapsulation of cells to increase the viability and local retention of cells when injected. Previous works have shown that hydrogels are promising alternatives to PBS for administration of cell therapies, as they enhance local retention and improve the viability of cells during injection when compared to injections performed in PBS.<sup>[10–22]</sup> It has been proposed that hydrogel “plug flow,” a phenomena caused by the rheology of these materials, protects the cells from the shear and extensional forces during injection from a syringe and needle.<sup>[11]</sup> Hydrogels may also be used to provide an ECM mimic to enhance cell growth and differentiation.<sup>[23]</sup>

The design of materials for use in 3D printing or cell transplantation therapies is constrained both by the properties required for injectability and terminal functionality.<sup>[17]</sup> Injectability requires that an acceptable flow rate of the hydrogel at the maximum pressure applicable by relevant personnel (i.e., health professional) is easily achieved. Injectability is affected by both the flow properties of the material and the conditions (i.e., flow rate, geometry) under which the injection is being performed. Terminal functionalities such as in cell injection applications may require formation of a localized “solid-like” depot after the hydrogel is injected for successful retention and localization of the cells in the target area. Therefore, the material is required to be liquid-like when administering through a needle yet solid-like after injection. To date, researchers have fit this seemingly contradictory and complex design envelope for

Dr. H. Lopez Hernandez  
Department of Materials Science & Engineering  
Stanford University  
Stanford, 94305 CA, United States

Prof. A. K. Grosskopf  
Department of Chemical Engineering  
Stanford University  
Stanford, 94305 CA, United States

L. M. Stapleton, G. Agmon  
Department of Bioengineering  
Stanford University  
Stanford, 94305 CA, United States

Prof. E. A. Appel  
Department of Materials Science & Engineering  
Department of Bioengineering  
Stanford University  
Stanford, 94305 CA, United States  
E-mail: eappel@stanford.edu

The ORCID identification number(s) for the author(s) of this article can be found under <https://doi.org/10.1002/mabi.201800275>.

DOI: 10.1002/mabi.201800275

cell delivery by developing i) covalently bound static materials such as hydrogels injected as low viscosity precursors that gel in situ<sup>[10]</sup> to form a localized cell environment; and ii) dynamic supramolecular systems such as hydrogels comprising host-guest moieties, peptide-functionalized polymers, and peptide amphiphiles<sup>[24–26]</sup> that employ shear-thinning to flow through needle. Supramolecular hydrogels are promising because they shear-thin and do not require in situ polymerizations.<sup>[4,13,27,28]</sup>

Recently, supramolecular hydrogels have seen an increase in application because they possess highly tunable mechanical properties, cargo diffusion kinetics, erosion kinetics, stimuli-responsiveness, chemical functionality, and increased injectability/printability.<sup>[24–26,29,30]</sup> Dynamic polymer–nanoparticle (PNP) interactions<sup>[31]</sup> have been utilized to create a hydrogel drug-delivery platform with shear-thinning rheological properties.<sup>[32–34]</sup> These PNP hydrogels are easily synthesized by mixing of dodecyl-modified hydroxypropylmethylcellulose (HPMC-C<sub>12</sub>) and PEG-*b*-PLA nanoparticles (NP), and are scalable, biocompatible, and exhibit yield-stress flow properties suited for the injection of cell depots.<sup>[32]</sup> Previous work has demonstrated the release of both hydrophobic and hydrophilic molecular cargo from the hierarchical gel structure, with Fickian diffusion release of cargo in the aqueous bulk and erosion release cargo loaded in the nanoparticles.<sup>[32]</sup> There is potential to expand the cargo loaded into PNP hydrogels to cells and enable the future codelivery of cells, drugs, and proteins with controllable release rates (Figure 1).

We injected cells with high cell viability in a PNP hydrogel, demonstrating successful encapsulation and compatibility between cells and the hydrogel. The yielding and shear-thinning of the hydrogel allowed for localized delivery and retention of cells while simultaneously allowing for facile low-pressure injection through 30-gauge needles.<sup>[35]</sup> hMSCs remained homogeneously dispersed in the hydrogel after 30 min of incubation at 37 °C and continued to proliferate in the hydrogel as rapidly as in hMSC media. Importantly, these supramolecular

hydrogels do not require an in situ gelation step after injection, are easily made, and are scalable for future clinical translation.

Yield-stress measurements were performed for a HPMC:NP hydrogel comprising 1 wt% HPMC-C<sub>12</sub> and 5 wt% PEG-*b*-PLA (denoted 1:5 HPMC:NP). An apparent yield stress of 30 Pa (Figure S1, Supporting Information) was measured at a rate of 1.45 Pa s<sup>-1</sup>. While yield-stress fluids are somewhat controversial,<sup>[35]</sup> the apparent yielding of the material is observed in the solid–liquid transition of the hydrogels as they pass through the high shear zone in the needle followed by a liquid–solid transition after the hydrogel is ejected as shown in Figure 2a.<sup>[36]</sup> 1:5 HPMC:NP hydrogels were easily injectable yet maintained a solid-like behavior after injection (Figure 2b).

A series of frequency sweeps of 1:5 HPMC:NP hydrogel and 1:1 HPMC:NP solution is shown in Figure 2c to demonstrate the solid-like behavior of the gel at rest and the fluid-like behavior of a non-gelling HPMC:NP formulation. The 1:5 HPMC:NP hydrogel has a tan δ (a measure of viscoelasticity), less than 1 (i.e.,  $G' > G''$ ), indicating solid-like behavior for a majority of the experimental frequencies measured (at frequencies > 0.03 Hz), and the non-gelling 1:1 HPMC:NP solution has a tan δ greater than 1 (i.e.,  $G'' > G'$ ) showing a dominant liquid-like response. Hydrogels that have a dominant solid-like behavior provide the necessary local retention and protection not afforded by saline solutions but required for cell delivery applications.

The viscosity of HPMC:NP hydrogels decreases drastically as the shear rate is increased (Figure 2d). While the viscosity of the 1:5 HPMC:NP hydrogel is 152 Pa s at a shear rate of 0.1 s<sup>-1</sup>, it decreases to 1 Pa s at a shear rate of 100 s<sup>-1</sup>. When fit to a power law model ( $\eta = K\dot{\gamma}^{n-1}$ ) for viscosity  $\eta$ , the shear-thinning parameter  $n$  is 0.41 with a consistency index  $K$  of 38 Pa s <sup>$n$</sup> . Importantly, the viscosity of the 1:5 HPMC:NP hydrogel approaches that of a 1:1 HPMC:NP viscous solution at higher shear rates and provides a relatively low resistance to flow regardless of its high viscosity and solid-like properties

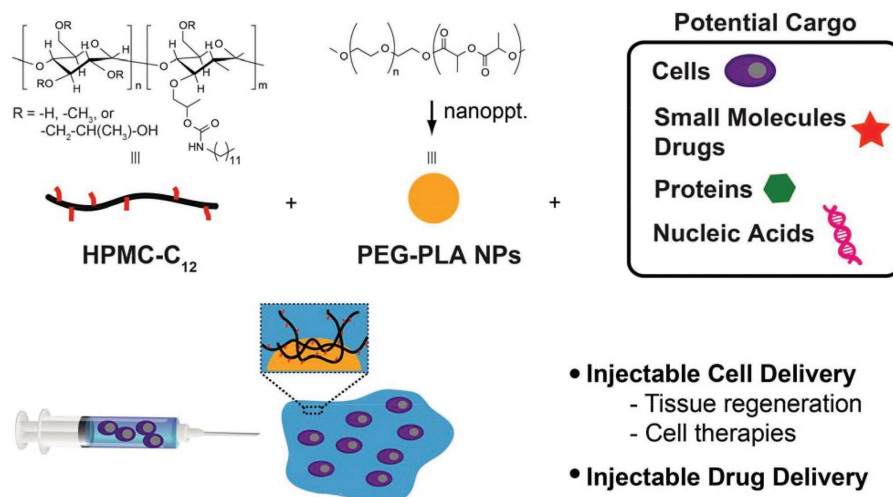


**Figure 1.** Tunable hydrogel platforms formed with physical polymer–nanoparticle interactions between cellulose derivatives and nanoparticles are injectable and shear-thinning, making them ideal for the encapsulation and delivery of proteins,<sup>[32]</sup> small molecules,<sup>[32]</sup> and, in this work, the protection of cells during injection.

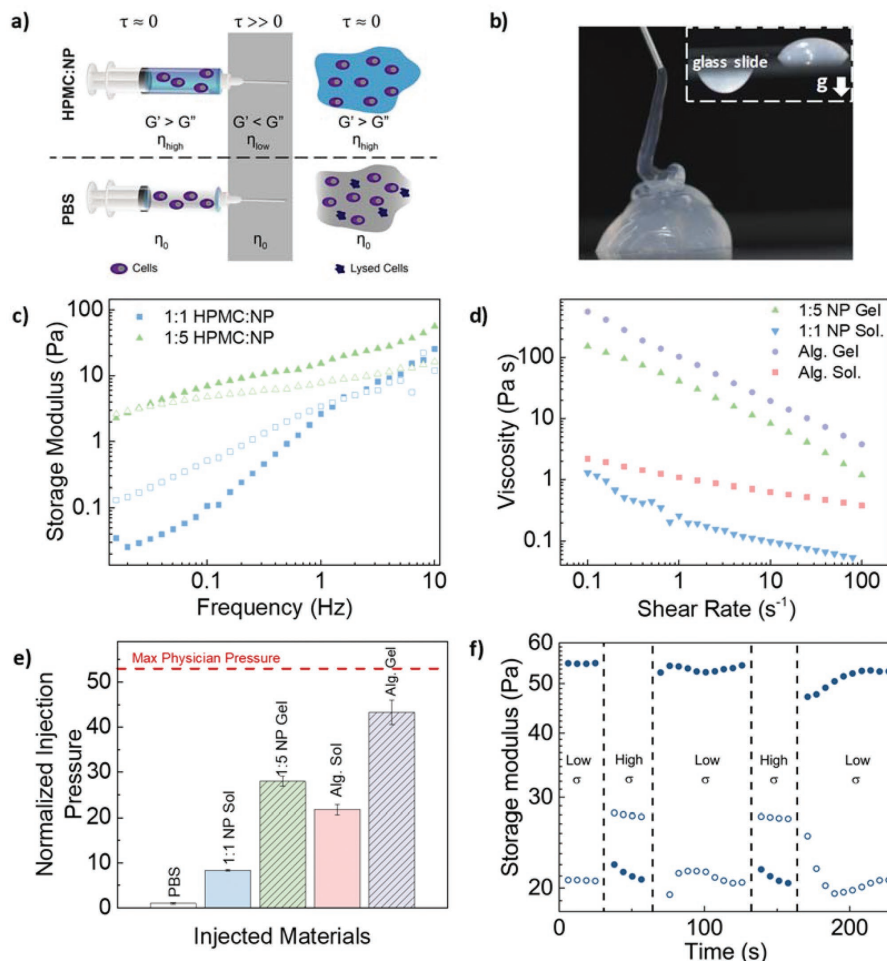


**Figure 2.** Rheology and Injectability of HPMC:NP hydrogel. a) The viability of injected cells is dependent on injection conditions and material properties of the fluid, where hydrogels have been demonstrated to increase injected cell viability. b) Demonstration of injectable HPMC:NP hydrogel injected from a 30-gauge needle and an inset demonstrating its resistance to flow. c) Frequency sweep of 1:5 (NP gel) and 1:1 (NP Sol.) HPMC:NP formulations ( $G'$ , closed symbols;  $G''$ , open symbols). d) Viscosity of HPMC:NP hydrogels compared to 2 wt% alginate ionically crosslinked with  $Ca^{2+}$  (25 mM  $Ca^{2+}$  Alg. Gel, 2.5 mM  $Ca^{2+}$  Alg. Sol.). e) Pressure required to inject different materials through a  $\frac{1}{2}$ "-long 30-gauge needle in a 5 mL glass syringe. Statistical significance determined by Student's *t*-test yielded  $p < 0.001$  for all comparison except 1:5 NP gel and Alg. Sol which yielded  $p < 0.05$ . f) Results from application of low and high stress amplitudes to the 1:5 HPMC:NP hydrogel demonstrating repeatable switching between fluid-like and solid-like properties.

at low stress. For comparison, viscosities of an alginate solution (2.5 mM  $Ca^{2+}$ , 2 wt% alginate) and an alginate hydrogel (25 mM  $Ca^{2+}$ , 2 wt% alginate) are also shown (frequency sweeps shown in Figure S2, Supporting Information). Ionically crosslinked alginate is a common hydrogel used for the delivery of cells and cargo that exhibits shear-thinning and has been demonstrated to increase the viability of injected cells.<sup>[11]</sup> It is apparent that the HPMC:NP hydrogels have similar rheological behavior to alginate, suggesting that HPMC:NP hydrogels may also protect cells from the shear forces applied during injection as shown for alginate hydrogel injections.

Injection pressures were measured to demonstrate the injectability of the hydrogels through a clinically relevant 30-gauge needle and for comparison to rheological properties. Injection pressures shown in Figure 2e were normalized

by the injection pressure required for PBS. The 1:1 HPMC:NP solution, 1:5 HPMC:NP hydrogel, 2.5 mM alginate solution, and 25 mM alginate hydrogel required 8, 28, 22, and 43 times more pressure for injection, respectively, than the PBS solution. The force profiles measured for each material are shown in Figure S4, Supporting Information. The hydrogels tested all required less pressure than the maximum pressure applicable by health personnel,<sup>[37]</sup> a necessary requirement for clinically relevant injectability.

The injectability of these supramolecular systems remained despite of the high viscosity at low shear rates (Table 1). If these materials did not shear-thin and were instead Newtonian fluids (e.g., water), the pressure required to drive fluid flow in a needle would be linearly proportional to the viscosity of the fluid. Since these hydrogels shear-thin, the required injection pressure

**Table 1.** Rheological properties of HPMC:NP and alginate materials.

Carrier material	$G'$ @ 1 Hz [Pa]	$G''$ @ 1 Hz [Pa]	$\eta$ @ 1 s <sup>-1</sup> [Pa s]	$n$	$K$ [Pa s <sup><math>n</math></sup> ]	Injection pressure [kPa]
1 wt% HPMC 1 wt% PEG- <i>b</i> -PLA	0.33 ± 0.01	1.2 ± 0.3	0.28 ± 0.01	0.30	0.20	125 ± 3.1
1 wt% HPMC 5 wt% PEG- <i>b</i> -PLA	16 ± 1.9	9.0 ± 1.2	38 ± 7.6	0.40	41	421 ± 17
2.5 mM Ca <sup>+</sup> 2 wt% Alginate	1.5 ± 0.5	2.6 ± 0.9	1.3 ± 0.67	0.68	0.20	327 ± 16
25 mM Ca <sup>+</sup> 2 wt% Alginate	810 ± 180	74 ± 12	97.6 ± 11	0.20	101	650 ± 42
PBS	—	—	1e-3	—	—	15 ± 2.3

depends on viscosity, shear-thinning index, yield stress, needle diameter, and flow rates. Therefore, it is impossible to predict injectability of a non-Newtonian fluid by only considering viscosity measured at a single shear rate.<sup>[38]</sup> For example, predictions using the Hagen–Poiseuille law with viscosities measured at 1 s<sup>-1</sup> would suggest that 1:5 HPMC:NP would require 38 000 times more pressure to inject than the PBS, yet the injection of 1:5 HPMC:NP only required 28 times more pressure.

A decrease in required injection pressure for shear-thinning fluids is a necessary property for injectable systems, allowing for facile injections by relevant personnel while maintaining the material properties required to perform as a cell delivery and retention platform. Each application however will require specific tailoring of the rheological properties to match the constraints of the intended application. For example, in catheters, the length of the capillary becomes very long when compared to a needle. As the length of a cylindrical tube is increased the pressure required to drive the fluid increases linearly which quickly results in injection pressures surpassing humanly applicable injection pressures. In these applications, careful consideration must be taken to engineer a material system that will remain injectable under the new design constraints.

After injection, the 1:5 HPMC:NP hydrogel rapidly recovers its solid-like properties as shown pictorially in Figure 2b and rheologically in Figure 2f. Here, the strain amplitude is increased past the yield point of the material and then decreased below it while measuring the materials stress response. The material quickly switches between solid-like and liquid-like states as it yields and recovers each cycle. In a flow experiment (Figure S3, Supporting Information), the viscosity is shown to drastically decrease at high shear rates and recover at low shear rates. As the material rapidly recovers, it retains its ability to localize the delivery of cells.

The effectiveness of the non-Newtonian 1:5 HPMC:NP hydrogel as a cell delivery material was evaluated for cell injections through a 30-gauge needle attached to a 1 mL syringe. Human umbilical vein cells (HUVECs), adult human dermal fibroblasts (HDFa), smooth muscle cells (SMCs), and human mesenchymal stem cells (hMSCs) were tested. Cells were injected at a concentration of 5 million cells mL<sup>-1</sup> and immediately tested with a Live/Dead assay (Figure 3a). Live/Dead assays were also performed on non-injected cells in both PBS and the 1:5 HPMC:NP hydrogel as controls.

Based on previous reports, PBS injections were expected to lead to significant cell death,<sup>[11]</sup> but it was found that the viability of injected cells was largely dependent on the cell type. HUVECs were the most sensitive to injection in PBS with an average viability of 68 ± 14%. When injected in the 1:5 HPMC:NP hydrogel, the viability of HUVEC was drastically increased to an average viability of 88 ± 9% with no significant difference from the non-injected hydrogel control group. HDFa were the most robust cell type tested, with no significant difference in the viability of cells after PBS injection. Injection from the hydrogel resulted in 93 ± 7%

viability, a 4% decrease from the non-injected hydrogel control group. SMCs experienced significant cell death with 84 ± 5% viability when injected in PBS, a 9% decrease of viable cells from the non-injected PBS group. Injecting SMCs in the hydrogel resulted in a viability of 86 ± 4%, a 4.5% decrease of viable cells from the non-injected hydrogel control group. hMSCs experienced significant cell death with 80 ± 6% viability when injected in PBS, a 12% decrease of viable cells from the non-injected PBS group. Injecting hMSCs in the hydrogel resulted in a viability of 93 ± 5%, a 2% decrease of viable cells from the non-injected hydrogel control group.

In all cases, cells injected with 1:5 HPMC:NP hydrogels are viable to a high degree with at least 86% viability, proving that 1:5 HPMC:NP hydrogels protect the cells during injection and do not have any adverse acute effects on cell viability. In the case of HUVECs injections, where a large quantity of dead cells was observed with PBS injections, the 1:5 HPMC:NP hydrogel significantly increased the viability of the injected cells by 20%. For SMCs and HDFa, it was difficult to identify a difference between PBS and hydrogel injection but the decrease in cell viability with hydrogel injections was minimal. Protection provided by 1:5 HPMC:NP hydrogels during injection is consistent with prior studies of cell viabilities in injection with shear-thinning materials,<sup>[11]</sup> supporting the hypothesis that non-Newtonian materials provide flow conditions through a needle/syringe that preserve cell viability. Furthermore, the cells in non-injected hydrogels were all measured at above 90% viability, confirming that the composition of the hydrogel (HPMC-C<sub>12</sub> and PEG-*b*-PLA NPs) and mixing the cells into hydrogel is not harmful to the cells.

hMSCs loaded into a 1:5 HPMC:NP hydrogel continued to proliferate as fast as hMSCs plated with cell media. Over the course of 7 days the metabolic activity, as measured by an MTS assay (Figure 3b), continued to increase for cells loaded in the hydrogel at a similar rate as cells plated with cell media. The hydrogel does not inhibit the growth of the hMSCs over the 7 day period and is a positive indicator that it may be compatible with future cell administration applications.

Given the non-Newtonian behavior of the 1:5 HPMC:NP hydrogel, we hypothesized that the yield stress of the hydrogel would serve to prevent any cell sedimentation after mixing. A settling assay was performed as reported by Dubbin et al.<sup>[13]</sup> A maximum projection confocal fluorescence image of hMSCs in a 1:5 HPMC:NP gel is shown in Figure 3c showing that they



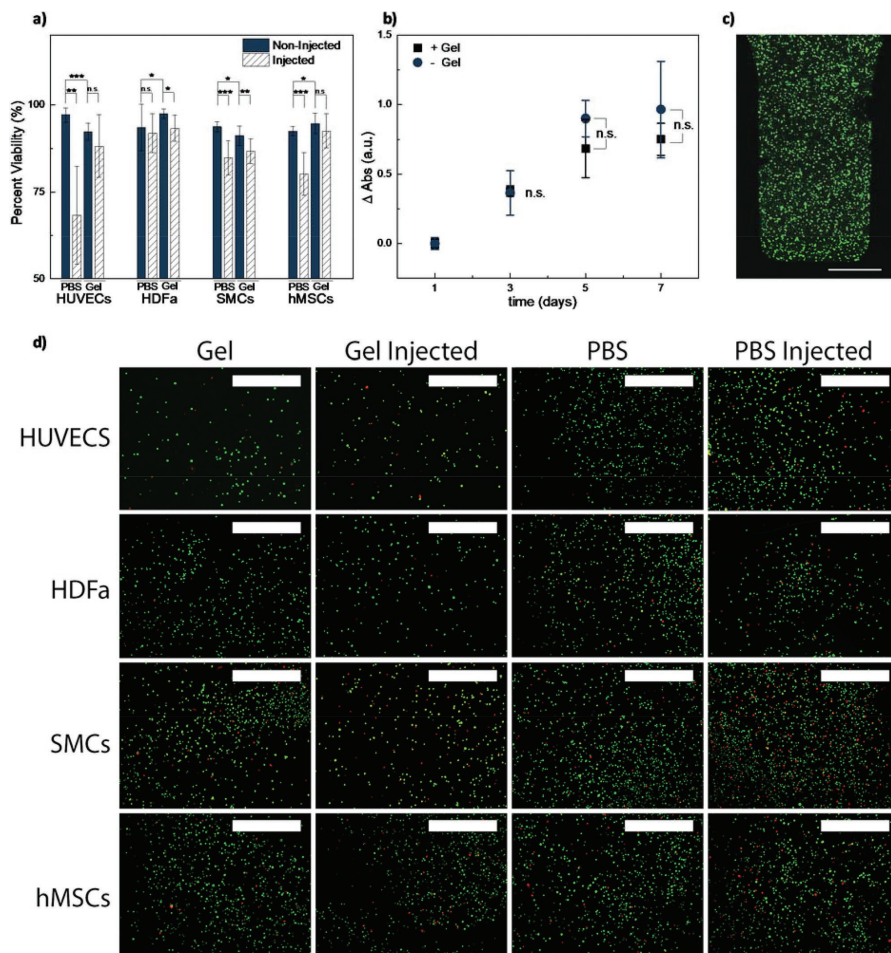


**Figure 3.** Injected cell viability. a) Cell viability in a Live/Dead cytotoxicity assay of HUVECS, HDFa, SMCs, and hMSCs. b) Week-long metabolic MTS assay of hMSCs injected in 1:5 HPMC:NP hydrogel and in cell media. Student's *t*-test yielded no significance for comparisons between hydrogel and media groups. c) Thirty-minute settling assay of hMSCs in 1:5 HPMC:NP hydrogel. Scale bar is 1 mm. d) Representative images of the Live/Dead stained cells. Scale bar is 1 mm.

did not settle over the course of 30 min of incubation at 37 °C.

A cell settling coefficient of 1.03 ( $\delta = \frac{\sum c_i^2}{(\sum c_i)^2}$ ) was calculated

and confirmed the homogenous distribution of the cells in the hydrogel. Incorporating the cells into this hydrogel system is simple, requiring only a one-step mixing process and resulting in a homogenous distribution of the cells. Furthermore, its ability to retain cells suspended for long times confirms that it will serve as an effective cell depot that retains cells at a site of injection without quickly releasing them through some flow process.

Here, polymer–nanoparticle hydrogels comprising dodecyl-modified HPMC and PEG-*b*-PLA nanoparticles (NP) are presented as a new platform for cell injection with several advantages over existing covalent hydrogel systems. The dynamic physical interactions between the HPMC and NP cause these materials to yield and shear-thin, whereby the microstructure is destroyed at high stresses and rapidly returns when the shear

stress is removed, making them easily injectable through clinically relevant needle gauges. It was demonstrated that a 1 wt% HPMC 5 wt% NP hydrogel allowed for high cell viability of injected HUVECS, HDFa, SMCs, and hMSCs immediately after being injected from a 30-gauge needle. The hydrogels are shown to suspend hMSCs and prevent sedimentation while allowing for proliferation of hMSCs over a 7 day period. Further work will explore HPMC:NP hydrogels as cell depots for the local retention, protection, and transport of cells when embedded in the body. This approach may lead to the enhancement of cell therapies by providing a safe local environment of injected cells and potentially the codelivery of other drugs or growth factors that could work in conjunction with cell delivery.

## Experimental Section

*Hydroxypropylmethylcellulose, PEG-b-PLA, and Alginate:* Dodecyl-modified hydroxypropylmethylcellulose (10% modified) and PEG-*b*-PLA



(5 kDa PEG, 20 kDa PLA) nanoparticles were made according to previously published protocols.<sup>[32]</sup> Alginate was synthesized at 2.5 mm and 25 mm Ca<sup>+</sup> according to previously published protocols.<sup>[39]</sup>

**Culture of Human Dermal Fibroblasts:** HDFa (Fisher) were cultured using DMEM (Fisher) supplemented with 10% fetal bovine serum (FBS, Fisher) and 1% penicillin–streptomycin (Fisher). The cells were incubated under 21% O<sub>2</sub>, 5% CO<sub>2</sub>, and 37 °C conditions. Cells between passages 8 and 12 were used for the studies.

**Culture of Smooth Muscle Cells:** SMCs (Lonza) were cultured using DMEM (Fisher) supplemented with 10% FBS (Fisher), and 1% penicillin–streptomycin (Fisher). The cells were incubated under 21% O<sub>2</sub>, 5% CO<sub>2</sub>, and 37 °C conditions. Cells between passages 3 and 6 were used for the studies.

**Culture of Human Umbilical Vein Endothelial Cells:** HUVECs (Lonza) were cultured using EGM growth medium supplemented with Endothelial Cell Growth Kit (Lonza). The cells were incubated under 21% O<sub>2</sub>, 5% CO<sub>2</sub>, and 37 °C conditions. Cells between passages 3 and 6 were used for the studies.

**Culture of Human Mesenchymal Stem Cells:** hMSCs (Fisher) were cultured using AlphaMEM (Fisher) supplemented with 10% FBS (Fisher) and 1% penicillin–streptomycin (Fisher). The cells were incubated under 21% O<sub>2</sub>, 5% CO<sub>2</sub>, and 37 °C conditions. Cells in passage 8 were used for the studies.

**Cell Injections and Live/Dead Assay:** HPMC:NP hydrogels are made by mixing a 20 wt% nanoparticle solution in PBS with dissolved HPMC. Cells were incorporated homogeneously into the gels ( $5 \times 10^6$  cells mL<sup>-1</sup>) by suspending the cells in the 20 wt% NP solution and then adding the NP solution to the viscous HPMC solution. The solutions were mixed gently in a microcentrifuge tube until the hydrogel was formed. Control samples were made in PBS alone at a cell concentration of  $5 \times 10^6$  cells mL<sup>-1</sup>. Injected specimens were loaded into a 1 mL syringe with a 30-gauge needle and then injected by hand at a flow rate between 1.2 and 2 mL min<sup>-1</sup>. PBS samples were directly injected or pipetted (control) into a centrifuge tube. Hydrogel samples were injected or pipetted (control) onto a glass slide and then dissolved in 13 mL of cell media by light agitation between two glass slides. All samples were centrifuged and the cell pellets resuspended in PBS for Live/Dead testing. A Live/Dead viability/cytotoxicity kit, for mammalian cells by Invitrogen (Thermo Fisher) was used to evaluate viability of cells immediately being injected. Cells were incubated at room temperature for 45 min with 2 mM calcein-AM and 4 mM ethidium homodimer-1 in PBS. After incubating, cells were covered with a cover glass and then imaged with an EVOS FL fluorescence microscope (Thermo Fisher). Samples sizes were at least equal to nine and statistical significance was determined using the Student's *t*-test.

**MTS Cell Proliferation Assay:** An MTS assay (Abcam) was used according to provided procedures to measure the proliferation of hMSCs in a 1:5 HPMC:NP hydrogel. Cells were mixed into the hydrogel as previously described and then 100  $\mu$ L of gel with 8000 cells was deposited into a 96-well plate. The hydrogels were covered by cell media and then incubated for 1, 3, 5, and 7 days. After the prescribed incubation time, the MTS reagents were added and fluorescence measured after 3.5 h of incubation. The proliferation of the hMSCs in the hydrogel was compared to the proliferation of the cells in hMSC media.

**Cell Settling Assay:** hMSCs were suspended in serum-free AlphaMEM with Calcein Cell Tracker and incubated at 37 °C for 15 min. Cells were then encapsulated at a concentration of 1.5 million cells mL<sup>-1</sup> into HPMC:NP hydrogels. 150  $\mu$ L of hydrogel was loaded into the bottom of cuvettes using a 25 G needle. After 30 min, cuvettes were laid on their side and imaged with a confocal microscope. The images were taken with a 10 $\times$  objective in 20  $\mu$ m increments for a total of 400  $\mu$ m of depth into the gel. The cuvettes were then reverted to the upright position and incubated at 37 °C until the imaging was repeated in 1 h and 4 h increments. Images were then created from the maximum intensity projection of the images for an area of 4.2 mm  $\times$  2.8 mm.

**Rheology:** Rheology measurements were performed on a TA instruments Discovery HR-2 rheometer using a 20 mm plate geometry. Frequency sweeps were performed at a constant torque of 2  $\mu$ N m

(1.27 Pa) from 0.1 to 100 rad s<sup>-1</sup>. Flow sweeps were performed at shear rates from 100 s<sup>-1</sup> to 0.01 s<sup>-1</sup>. Stress ramps were performed at 1.45 Pa s<sup>-1</sup>. Dynamic self-healing experiments were performed by switching between 0.17 Pa and 525 Pa at a frequency of 10 rad s<sup>-1</sup> and 60 s and 30 s intervals, respectively.

**Injections Pressure Measurements:** Injection pressures were measured using a load cell attached to a syringe pump. The load cell was purchased from FUTEK model LLB300 and has a capacity of 222.4 N. The syringe pump was purchased from KD Scientific model Legato 100. LabView 2017 was used to simultaneously monitor the load required during injection. Injections were performed at 1 mL min<sup>-1</sup> using a 5 mL glass syringe and 30-gauge 0.5 in needle. Reported pressure values are averaged from the plateau region of the injection pressure measurement. While the syringe used in cell injections was a 1 mL syringe and the syringe used for pressure measurements was a 5 mL syringe, it is important to highlight that the size of the syringe has a negligible impact on the injectability of the hydrogel (Figure S4, Supporting Information).

## Supporting Information

Supporting Information is available from the Wiley Online Library or from the author.

## Acknowledgements

This project was funded by the Terman Faculty Fellowship and the Stanford BIOX Interdisciplinary Initiatives Program (2016) Seed Grant. H.L.H. is thankful for funding provided by the NSF ACEP California Alliance Postdoctoral Fellowship. A.K.G. is extremely grateful for financial support from the Gabilan Fellowship of the Stanford Graduate Fellowships Program. G.A. and L.M.S. are thankful for the support from the National Science Foundation Graduate Research Fellowship Program (DGE-1147470).

## Conflict of Interest

The authors declare no conflict of interest.

## Keywords

cell delivery, cell viability, non-Newtonian fluids, polymer–nanoparticle interactions, supramolecular hydrogels

Received: July 23, 2018  
Revised: September 28, 2018  
Published online:

- [1] M. W. Tibbitt, J. E. Dahlman, R. Langer, *J. Am. Chem. Soc.* **2016**, *138*, 704.
- [2] J. Li, D. J. Mooney, *Nat. Rev. Mater.* **2016**, *1*, 16071.
- [3] P. S. Gungor-Ozkerim, I. Inci, Y. S. Zhang, A. Khademhosseini, M. R. Dokmeci, *Biomater. Sci.* **2018**, *6*, 915.
- [4] H. Wang, S. C. Heilshorn, *Adv. Mater.* **2015**, *27*, 3717.
- [5] M. W. Tibbitt, K. S. Anseth, *Sci. Transl. Med.* **2012**, *4*, 160ps24.
- [6] R. Dimatteo, N. J. Darling, T. Segura, *Adv. Drug Delivery Rev.* **2018**, *127*, 167.
- [7] A. A. Foster, R. E. Dewi, L. Cai, L. Hou, Z. Strassberg, C. A. Alcazar, S. C. Heilshorn, N. F. Huang, *Biomater. Sci.* **2018**, *6*, 614.



- [8] A. N. Steele, L. Cai, V. N. Truong, B. B. Edwards, A. B. Goldstone, A. Eskandari, A. C. Mitchell, L. M. Marquardt, A. A. Foster, J. R. Cochran, S. C. Heilshorn, Y. J. Woo, *Biotechnol. Bioeng.* **2017**, *114*, 2379.
- [9] L. L. Wang, Y. Liu, J. J. Chung, T. Wang, A. C. Gaffey, M. Lu, C. A. Cavanaugh, S. Zhou, R. Kanade, P. Atluri, E. E. Morrissey, J. A. Burdick, *Nat. Biomed. Eng.* **2017**, *1*, 983.
- [10] X. Tong, F. Yang, *Adv. Healthcare Mater.* **2018**, *7*, 1701065.
- [11] B. A. Aguado, W. Mulyasmita, J. Su, K. J. Lampe, S. C. Heilshorn, *Tissue Eng., Part A* **2012**, *18*, 806.
- [12] T. Xu, J. Jin, C. Gregory, J. J. Hickman, T. Boland, *Biomaterials* **2005**, *26*, 93.
- [13] K. Dubbin, A. Tabet, S. C. Heilshorn, *Biofabrication* **2017**, *9*, 044102.
- [14] M. H. Amer, F. R. A. J. Rose, K. M. Shakesheff, L. J. White, *Stem Cell Res. Ther.* **2018**, *9*, 39.
- [15] X. Chen, A. G. Foote, S. L. Thibeault, *Cytotherapy* **2017**, *19*, 1522.
- [16] S. J. Bidarra, C. C. Barrias, P. L. Granja, *Acta Biomater.* **2014**, *10*, 1646.
- [17] M. H. Chen, L. L. Wang, J. J. Chung, Y.-H. Kim, P. Atluri, J. A. Burdick, *ACS Biomater. Sci. Eng.* **2017**, *3*, 3146.
- [18] C. B. Highley, C. B. Rodell, J. A. Burdick, *Adv. Mater.* **2015**, *27*, 5075.
- [19] T. Xu, K. W. Binder, M. Z. Albanna, D. Dice, W. Zhao, J. J. Yoo, A. Atala, *Biofabrication* **2013**, *5*, 015001. <https://doi.org/10.1088/1758-5082/5/1/015001>
- [20] T. Jungst, W. Smolan, K. Schacht, T. Scheibel, J. Groll, *Chem. Rev.* **2016**, *116*, 1496.
- [21] T. Billiet, E. Gevaert, T. De Schryver, M. Cornelissen, P. Dubruel, *Biomaterials* **2014**, *35*, 49.
- [22] C. M. Madl, S. C. Heilshorn, H. M. Blau, *Nature* **2018**, *557*, 335.
- [23] C. M. Madl, S. C. Heilshorn, *Adv. Funct. Mater.* **2018**, *28*, 1706046.
- [24] J. L. Mann, A. C. Yu, G. Agmon, E. A. Appel, *Biomater. Sci.* **2018**, *6*, 10.
- [25] M. J. Webber, E. A. Appel, E. W. Meijer, R. Langer, *Nat. Mater.* **2016**, *15*, 13.
- [26] E. A. Appel, J. del Barrio, X. J. Loh, O. A. Scherman, *Chem. Soc. Rev.* **2012**, *41*, 6195.
- [27] A. Sabnis, M. Rahimi, C. Chapman, K. T. Nguyen, *J. Biomed. Mater. Res., Part A* **2009**, *91A*, 52.
- [28] M. Guvendiren, H. D. Lu, J. A. Burdick, *Soft Matter* **2012**, *8*, 260.
- [29] E. A. Appel, R. A. Forster, M. J. Rowland, O. A. Scherman, *Biomaterials* **2014**, *35*, 9897.
- [30] E. A. Appel, X. J. Loh, S. T. Jones, C. A. Dreiss, O. A. Scherman, *Biomaterials* **2012**, *33*, 4646.
- [31] S. Rose, A. PrevotEAU, P. Elzière, D. Hourdet, A. Marcellan, L. Leibler, *Nature* **2014**, *505*, 382.
- [32] E. A. Appel, M. W. Tibbitt, M. J. Webber, B. A. Mattix, O. Veisoh, R. Langer, *Nat. Commun.* **2015**, *6*, 6295.
- [33] E. A. Appel, M. W. Tibbitt, J. M. Greer, O. S. Fenton, K. Kreuels, D. G. Anderson, R. Langer, *ACS Macro Lett.* **2015**, *4*, 848.
- [34] A. C. Yu, H. Chen, D. Chan, G. Agmon, L. M. Stapleton, A. M. Sevit, M. W. Tibbitt, J. D. Acosta, T. Zhang, P. W. Franzia, R. Langer, E. A. Appel, *Proc. Natl. Acad. Sci.* **2016**, *113*, 14255.
- [35] H. A. Barnes, *J. Non-Newtonian Fluid Mech.* **1999**, *81*, 133.
- [36] A. K. Grosskopf, R. L. Truby, H. Kim, A. Perazzo, J. A. Lewis, H. A. Stone, *ACS Appl. Mater. Interfaces* **2018**, *10*, 23353.
- [37] W. Hayward, L. Haseler, L. Kettwich, A. Michael, W. Sibbitt, A. Bankhurst, *Scand. J. Rheumatol.* **2011**, *40*, 379.
- [38] R. A. Chilton, R. Stainsby, *J. Hydraul. Eng.* **1998**, *124*, 522.
- [39] K. Wisdom, O. Chaudhuri, *Methods Mol. Biol.* **2017**, *1612*, 29.